Geomechanics and Engineering, *Vol. 14, No. 5 (2018) 459-466*
DOI: https://doi.org/10.12989/gae.2018.14.5.459

Dilatation characteristics of the coals with outburst proneness under cyclic loading conditions and the relevant applications

Yangyang Li[1a], Shichuan Zhang[*1] and Baoliang Zhang[2b]

[1]*State Key Laboratory of Mining Disaster Prevention and Control, Shandong University of Science and Technology, Shandong 266590, China*
[2]*College of Architecture Engineering, Liaocheng University, Shandong 252000, China*

(Received January 7, 2017, Revised September 12, 2017, Accepted September 18, 2017)

Abstract. By conducting uniaxial loading cycle tests on the coal rock with outburst proneness, the dilatation characteristics at different loading rates were investigated. Under uniaxial loading and unloading, the lateral deformation of coal rock increased obviously before failure, leading to coal dilatation. Moreover, the post-unloading recovery of the lateral deformation was rather small, suggesting the onset of an accelerated failure. As the loading rate increased further, the ratio of the stress at the dilatation critical point to peak-intensity increased gradually, and the pre-peak volumetric deformation decreased with more severe post-peak damage. Based on the laboratory test results, the lateral deformation of the coals at different depths in the #1302 isolated coal pillars, Yangcheng Coal Mine, was monitored using wall rock displacement meter. The field monitoring result indicates that the coal lateral displacement went through various distinct stages: the lateral displacement of the coals at the depth of 2-6 m went through an “initial increase-stabilize-step up-plateau” series. When the coal wall of the working face was 24-18 m away from the measuring point, the coals in this region entered the accelerated failure stage; as the working face continued advancing, the lateral displacement of the coals at the depth over 6 m increased steadily, i.e., the coals in this region were in the stable failure stage.

Keywords: rock mechanics; different loading rates; stress-strain curve; coal dilatation; lateral deformation

1. Introduction

In coal mining process, due to the concerns over geological conditions, above-ground buildings and mine disasters, large number of fault, strip and corner coal pillars are usually left behind, which may be subject to concentrated high stress after repeated mining. Thus, during coal pillar mining or haulageway digging near the pillar, the coals in the mining area could be largely deformed, which may trigger dynamic hazards like rock bursts and coal/gas outbursts. A great number of studies have shown that, under cyclic loading, rocks exhibit different strength and deformation characteristics from those in uniaxial compression tests. Xie *et al.* (2014) studied the fatigue crack growth behavior of a kind of fiber metal laminates (FML) under four different stress levels, and found that the maximum stress level has an almost linear relationship with the stress intensity factor. Heap and Faulkner (2008) investigated and quantified the contribution of micro cracking to the static elastic response of Westerly granite by increasing-amplitude cyclic loading and constant-amplitude cyclic loading experiments. In the light of the localized progressive damage model and constitutive model, Qiu *et al.* (2015) indicated that the essential failure mechanism of the cracked rock can be described by the cohesion weakening and friction strengthening evolution law.

Zhou *et al.* (2010) focused on the mesomechanics of the microscopic cracks in the sandstones from Xiangjiaba Dam, and investigated their stress-strain curve and failure characteristics in fracture mechanics under uniaxial cyclic loading conditions; Xiao *et al.* (2010) conducted constant-amplitude cyclic loading tests on granite and explored their deformation characteristics.

The variation rate of rock loading induced by engineering construction, loading and tectonic compression signifies the engineering importance of the study on the effect of strain rate on rock’s mechanical properties (Mouthereau *et al.* 2009). Therefore, rock load variation rate has always been a focus point in both academic and engineering circles, with many results, especially in dynamic/impact loading as well as fracture failure tests. Based on previous research results, Welander and Snygg (2009) obtained statistics of the loading strain rate (10^{-4}-10^{-8} s^{-1})effects in dolomite, limestone, granite and basalt under loading tests. According to their conclusions, when the loading strain rate increased from 10^{-6} s^{-1} to 10^{-3} s^{-1}, peak intensity increased significantly with it; as the loading strain rate went further up over 10^{-6} s^{-1}, peak intensity tended to stabilize. Zhou *et al.* (2009) performed the three-point bending tests on limestones and revealed the effect of loading rate(10^{-4}-10 mm/s) on the critical strain energy of

∗Corresponding author, Ph.D.
E-mail: 373260186@qq.com
[a]Ph.D.
E-mail: 1161826089@qq.com
[b]Ph.D. Student
E-mail: 996457633@qq.com

ISSN: 2005-307X (Print), 2092-6219 (Online)

the unstable fracture propagation. EA Lyamina (2016) investigated the strain rate (5×10^{-7}-1×10^{-5} s^{-1}) effect on peak intensity of the rocks with different porosities and saturabilities, and found that the rock's peak intensity increased with the creep strain rate. Huang *et al.* (2012) performed uniaxial compression tests on coarse marbles at nine different loading rates within the static loading range to assess the rock's mechanical properties including failure mode, intensity and elastic modulus at different loading rates. HL Wang. (2011) examined the effects of strain rate on red sandstone's progressive failure process and characteristic stress. In all these previous studies, the scholars focused on the hard, dense and homogeneous rocks such as marble, granite and red sandstone, and carried out extensive experiments on their strengths and deformation characteristics under cyclic loading or at different loading rates (Jorat *et al.* 2013). However, no systematic research has been conducted so far on low strength coal rocks with lots of pre-existing damage.

Dilatation is an important mechanical feature of coal rocks. The emergence of rigid tester has provided a necessary premise for research on rock's post-peak (also known as post-failure) behaviors such as dilatation. Under a small confining pressure in uniaxial or triaxial loading, coal rocks undergo obvious dilatation, which is the key to damage and even collapse of coal rocks. According to laboratory test results, rock's dilatation, which appears before the peak and eventually disappears after the peak, shows distinct nonlinear characteristics, depending mostly on the variations of plastic strain and confining pressure (Zhao *et al.* 2015, 2010, Chai *et al.* 2014). This is in agreement with the mechanical response of the wall rocks around the excavation boundary of underground engineering. In order to accurately describe the rock's post-peak dilatation behavior, Huang *et al.* (2012) proposed the relevant theoretical and mathematical models and verified them in practical applications. Based on uniaxial cyclic loading test result of granite, Xiao *et al.* (2010) compared six damage variables and listed their respective advantages/disadvantages. Furthermore, Qiu *et al.* (2014) proposed the incremental cyclic loading test method and did quantitative analysis on the pre-peak damage behaviors of Jinping Marble. The above-described studies laid the emphasis on the rocks' elastic parameters, strength parameters and the quantitative descriptions of damage under cyclic loading conditions, while few studies on the coal rock' post-peak dilatation behaviors and fractures development process have been reported.

In the aspect of rock dilatancy, Zhang *et al.* (2016) develop a partial triaxial compression test to characterize the dilatancy of asphalt mixtures, he found that the degree of dilatancy changed with the strain ratio, which is sensitive to the air void content and loading rate. Kong *et al.* (2016) found that a hyperbolic relationship exists between the input plastic work and the particle breakage for Zipingpu gravel, regardless of the initial void ratio or the confining pressure under both monotonic andcyclic loading. Most of studies focused on rocks' dilatation mechanisms, without touching on the prediction of coal rock dilatation and rock-burst. Dilatation alters the coal rock's original occurrence state in the form of an abrupt change in the displacement parameters inside and outside the coal rock, which is an early sign of the occurrence of rock bursts. Therefore, the research on coal dilatation near the working face is of great significance for understanding the coals' rock burst mechanisms and effective prediction and prevention.

By conducting cyclic loading tests on 3rd coal seam, Yangcheng Coal Mine, Luneng Coal Industry & Electric Power Co., Ltd., coal rock' stress-strain curve pattern, dilatation properties and macroscopic failure characteristics under different loading rates were investigated and the internal relation between coal rock dilatation and lateral strain under cyclic loading conditions analyzed. The lateral deformation of coals at different depths in #1302 isolated coal pillar, Yangcheng Coal Mine, was then monitored, and the feasibility and reasonability of the prediction of coal damage/failure based on the monitored lateral deformation characteristics at different depths were examined.

2. Materials and methods

2.1 Sample preparation and test scheme

The coal rocks in the 3rd coal seam, #1302 working face, Yangcheng Coal Mine, were selected in this study. According to the identification results by Rock Mechanics Laboratory, China Coal Research Institute (CCRI), the 3rd coal seam of Yangcheng Coal Mine exhibits weak outburst proneness.

The intact and unweathered coal rock was selected and sealed on site, before being carried back to the laboratory for processing. According to the standards formulated by the International Society for Rock Mechanics, the coal rock was processed into the standard samples of Φ50 mm×100 mm. The coal sample surface was then polished by a sander, so that the parallelism between two sides was kept within ±0.02 mm. Fig. 1 shows the picture of the coal rock samples.

The tests were conducted on the servo test system (MTS815.03) in Shandong University of Science and Technology (see Fig. 2). The maximum axial load of the test system is 4600 kN, and the lateral and longitudinal ranges of the uniaxial extensometer are ±4 mm and -2.5-+12.5 mm, respectively. During the tests, the rock's lateral deformation was measured with the elongation of the ring-like chain wound around the sample center.

Fig. 1 Picture of coal rock samples

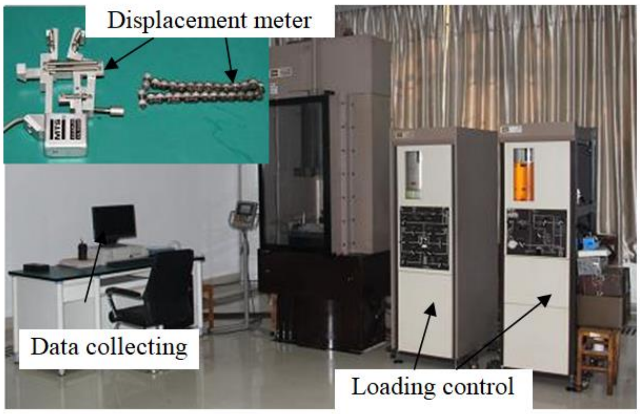

Fig. 2 MTS815.03 test system

Table 1 Basic physical and mechanical parameters of coal rock samples

Sample ID	Longitudinal wave velocity V/ (m · s^{-1})	Peak intensity /MPa	Modulus of elasticity E /GPa	Peak strain /10^{-3}
YCM-c1	1876.1	21.05	3.20	11.46
YCM-c2	1838.7	22.70	3.27	11.24
YCM-c3	1890.5	24.10	3.18	10.72

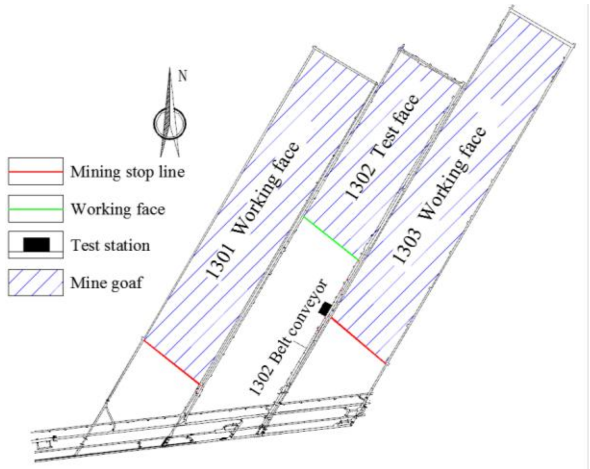

Fig. 3 Relative position of the working face and the arrangement of measuring points

Conventional uniaxial compression tests were first conducted on coal rock samples, with the results shown in Table 1. Different loading rates (v = 1 kN/s, 2 kN/s, 3 kN/s and 4 kN/s, respectively) were used with the set force goes up progressively with per cycle increments of 10 kN (i.e., the loading was applied in the sequence of 0.5→10→0.5→20→0.5→30 KN) until the sample was totally destroyed. Three samples were selected in each test.

2.2 Field monitoring scheme of coal lateral deformation

2.2.1 Selection of field test site

#1302 isolated working face, Yangcheng Coal Mine, was selected as the monitoring site in this study. Fig. 3 displays the relative position of #1302 working face, which

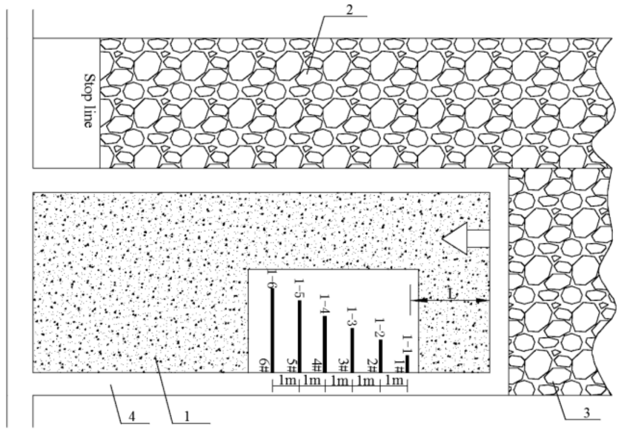

Fig. 4 Plan sketch of coal lateral deformation monitoring (Coals in working face/Goaf in the adjacent working face/Goaf in the current working face/Groove of the working face/L denotes the distance between the monitoring point and the coal walls of the working face, which is determined with the field monitoring data/1#, 2#, ...6# denote the monitoring holes at different depths/1-1, 1-2,....1-6 denote the lateral monitoring points at different depths)

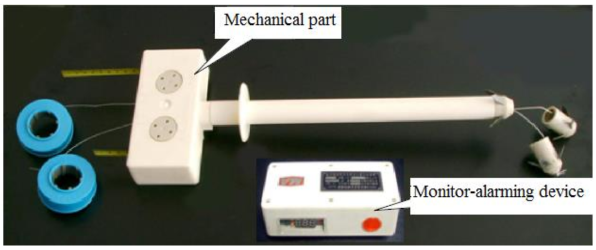

Fig. 5 Picture of the YHW300-range intrinsically safe wall rock displacement meter

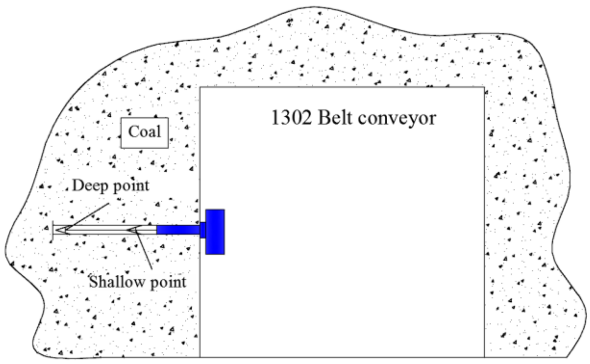

Fig. 6 Illustration of the field installation of the coal lateral deformation monitor

includes three coal seams. The coal seams exhibit rockburst proneness, with a hardness coefficient of 1.5, which puts them in the category of medium-hard coal seam. The angle of dip ranges from 17° to 25°, with an average value of 21°, and the thickness of coals ranges from 6.8 to 8.1 m, with an average value of 7.5 m. As to the working face, the burial depth is 440-50 m, the working face length is 191 m and the advance length is 912 m. Fully mechanized top coal caving method was used in #1302 working face, while the roof was

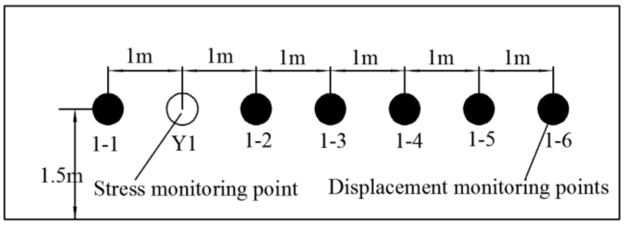

Fig. 7 Arrangement of coal lateral deformation monitoring station

Table 2 Installation depths of the monitor

Monitoring point	Shallow base point	Dark base point	Monitoring point	Shallow base point	Dark base point
1-1	2	3	1-4	6	8
1-2	3	4	1-5	8	10
1-3	4	6	1-6	9	10

managed with complete cave-in method. The caving height is 4.7 m, with a mining-to-caving ratio of 1:1.68. Cave-for-every-mining and two-round caving was used, with a step pitch of 0.8 m. The immediate roof of the coal seam is composed of medium sandstones, with a thickness of 12.98m; the main roof is composed of fine sandstones, with a thickness of 17.5 m; the immediate bottom is composed of mudstones, with a thickness of 1.61 m.

2.2.2 Monitoring method of coal lateral deformation

To investigate the lateral dynamic deformation rules of coals at a same position but different depth, the monitoring method for coal pillar as described in Ref. (Chen *et al.* 2012, Wang *et al.* 2013) was used. The lateral deformation monitors were installed along the groove of working face. The measuring points were set outside the range of abutment pressure in the working face at certain distances away from the stopping line. As shown in Fig. 4, the monitoring station is composed of 6 monitoring points(1-1, 1-2, 1-3, 1-4, 1-5,1-6), each monitoring point can monitor the lateral deformation of different depths of the coal. In order to avoid the influence of mining induced stress, the monitor should be installed outside support pressure outside the scope of abutment pressure, and there is a certain distance from the stop line. With the actual monitoring result, the maximum abutment pressure range of No.1 working face is 120 m. Therefore, the distance of the monitoring station from the coal wall is 133 m, from the stop line is 186 m

As shown in Fig. 5, the wide-range self-securing wall rock displacement meter (YHW300) was used for monitoring coal lateral deformation. This wall rock displacement meter consists of sensor and flukes connected by a 0.7 mm diameter steel wire rope. The resistance-type displacement sensor was used. When the wall rock displacement is detected, the flukes at different depths, via the steel wire rope, would pull the coil spring, which then would rotate the potentiometer. The change in the resistance of the precise rotational potentiometer generates a linearly varying voltage signal output, which is then converted to displacement via a transmitter before finally displayed digitally. Each wall rock displacement meter only measures the lateral deformation at two depths, and the relative deformation between the two lateral deformations could be output. The maximum range of the meter is 800 mm. The two depths monitored by each meter are, namely, the deep base point and the shallow base point, respectively. Fig. 6 illustrates the field installation of the wall rock displacement tester.

2.2.3 Arrangement of the coal lateral deformation monitoring points

Fig. 7 shows the arrangement of coal lateral deformation monitors. The monitoring station consists of six monitoring points at a spacing of 1 m. Table 2 lists the actual installation depths of the monitors.


(a) V = 1 kN/s


(b) V = 2 kN/s


(c) V = 3 kN/s


(d) V = 4 kN/s

Fig. 8 Coal rock's macroscopic failure modes under cyclic loading at different rates (V)

3. Results and Discussion

3.1 Coal rock' dilatation and loading rate effect under cyclic loading condition

3.1.1 Coal rock' macroscopic failure characteristics at different loading rates

Fig. 8 displays the rock's macroscopic failure patterns under cyclic loading at different rates. The following four failure modes are observed at different loading rates: (1) shear tension and splitting failure, i.e., an oblique shear plane appeared across the sample and several tensile failure faces appeared at the end of the sample; (2) splitting block failure, i.e., several penetrating splitting planes appeared, which were crosslinked to form small block failures; (3) splitting popping failure, i.e., several penetrating splitting surface appeared, accompanied by the popping of flaky or thin-block pieces, leaving behind dents on the surface of sample; intermittent crackles in the coal rock were also clearly heard; (4) popping failure, i.e., the thin-block or small grain pieces were ejected at a large velocity with continuous crackles.

3.1.2 Stress-strain curves of coal rock under cyclic loading tests

Fig. 9 shows the coal rock's stress-strain curve under cyclic loading tests at the rate of 1 kN/s. As the loading cycle times went on, the stress-strain hysteresis loop shifted towards the right hand side gradually. Before the rock got close to its failure point, the lateral strain was significantly smaller than the axial strain, so was its increasing rate as compared with that of axial strain as the loading cycle times went on; therefore the volumetric strain at this time was dominated by the axial strain, and the volume of coal rock actually decreased gradually. Right before the failure, the lateral strain increased rapidly, and was only slightly recovered after unloading, indicating an irreversible deformation in coal rock. This lead to a significant increase of volumetric strain, i.e., dilatation occurred in coal rock. According to the stress-strain curve, the significant increase of lateral strain followed by a small subsequent recovery upon unloading signals the entry into the accelerated failure stage.

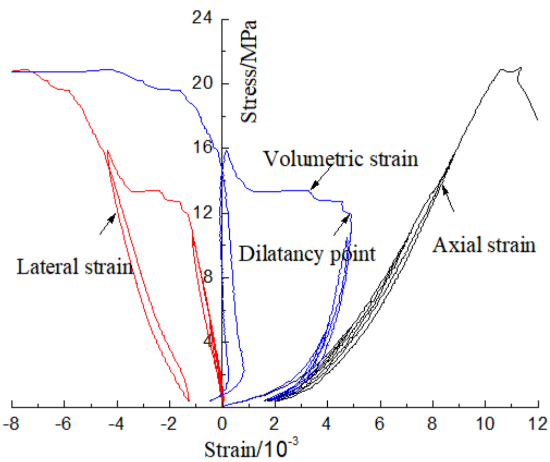

Fig. 9 Coal rock' stress-strain curves under cyclic loading at the rate of 1 kN/s

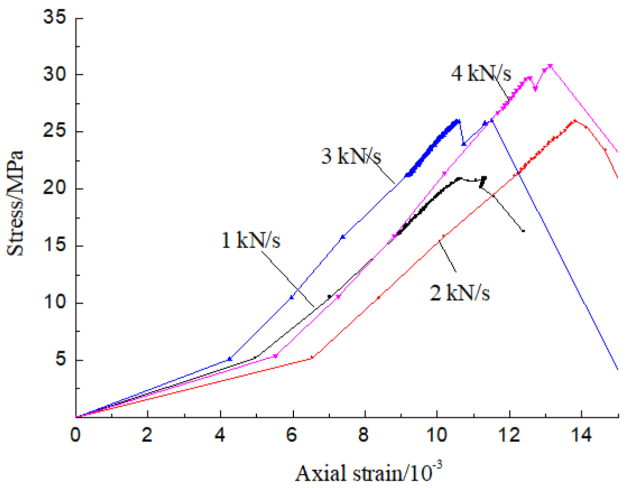

(a) Stress-axial strain

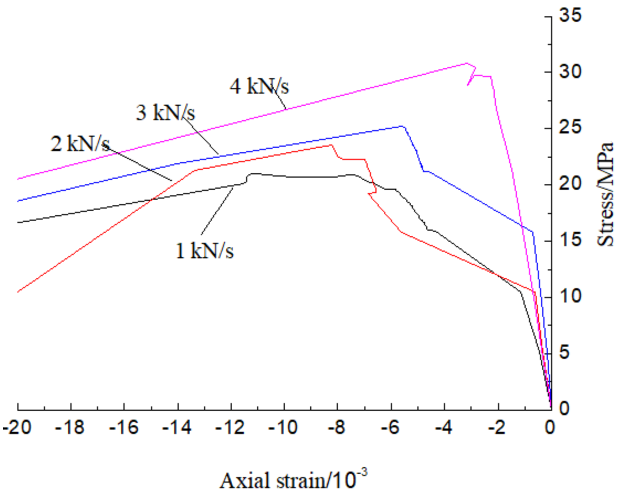

(b)Stress-lateral strain

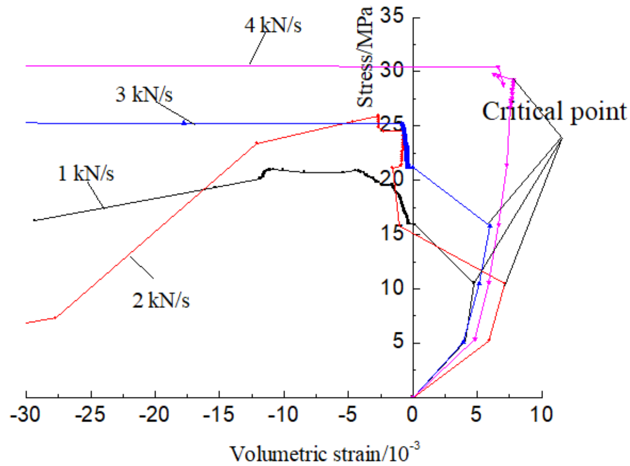

(c)Stress-volumetric strain

Fig. 10 Coal rock' stress-strain curves under cyclic loading at different loading rates

3.1.3 Dilatation characteristics of coal rock at different loading rates

Fig. 10 shows coal rock' stress-strain curves under cyclic loading at different loading rates The stress-axial strain curves at different loading rates almost follow the same rules with little dependence on loading rate. By contrast, the stress-lateral strain curves are significantly affected by the loading rate. At the beginning of loading, the coal rock exhibited similar lateral deformation at different loading rates. As we all know, numerous preexisting fractures, which vary in number, size and distribution, existed in the coal rock. Under a small external force, these preexisting fractures tend to close, leading to a greater difference in lateral strain. In the stage of accelerated failure, these fractures that have been closed are opened again, and many new fractures are generated; these fractures develop gradually and interconnect with each other, giving rise to the gradual increase of lateral strain. Moreover, with the increase of loading rate, the coal rock's lateral strain decreases with an increasing rate. In the post-peak failure stage, the fractures in the coal rock are interconnected to form large fractures, so that the lateral strain increases rapidly. As the loading rate decreases, the slope of stress-lateral strain curve decreases, indicating a more severe damage inside the coal rock.

As the loading rate increases, the stress at the dilatation critical point increases gradually, with values of 10.46 MPa, 10.52 MPa, 15.80 MPa and 28.81 MPa at the loading rate of 1 kN/s, 2 kN/s, 3 kN/s and 4 kN/s, respectively, and the ratio of the stress at the dilatation critical point to peak stress also increases steadily, with values of 50.1%, 51.4%, 62.4% and 93.5% at different loading rates, respectively. With increasing loading rate, the volumetric deformation from the dilatation critical point to peak-intensity point decreases. As stated above, a great number of preexisting fractures existed in the coal rock; under external force, these preexisting fractures and newly-generated fractures develop and interconnect, finally leading to the failure of coal rock. At a large loading rate, the fractures in coal rock have no adequate time to develop and expand, thus producing a smaller deformation before failure.

Fig. 11 is the relation between strain evolution and cycles number of coal under different loading rates. From this Fig., it can also be observed that loading rate has little effects on the e coal rock' strain curves pattern. Regardless of the loading rate, as long as it is within a certain range, the dilatation begins in the pre-peak yielding stage and becomes more significant after peak under uniaxial cyclic loading condition. Before the dilatation point, the axial strain is great while the lateral strain is relatively small; the coal rock volume is more affected by axial strain. After the dilatation point, the lateral strain increases rapidly while the axial strain increases at a relatively low rate; the coal rock volume is mainly affected by lateral strain.

The investigation results on coal rock' volumetric strain under tri-axial compression tests showed that, the coal rock expanded significantly under a small confining pressure; however, as the confining pressure increased, the coal rock shrank gradually. During the haulageway digging or working face mining process, the confining pressure is smallest at the extraction boundary of haulageway or the coal walls of the working face. Therefore, when the external force exceeded the stress corresponding to dilatation critical point, expansion of coals to the greatest degree and the maximum displacement towards free face would inevitably occur, eventually leading to coal collapse.

3.2 Field monitoring results and analysis

In this study, the lateral deformations of the coals at different depths in the coal walls of the #1302 isolated working face, Yangcheng Coal Mine, were monitored and the relation between lateral deformation and the mining face advancing was acquired and shown in Fig. 12. No monitoring data were collected for the 1-5# and 1-6# monitoring points due to installation and human issues. It can be seen that, when the working face coal wall was approximately 80 m away from the monitoring point, the lateral displacement was quite obvious in the region at 3~4 m depth at the 1-2# measuring point, indicating that the mining-induced stress in the working face first was already acting on the coals in this region; when the working face was 62-45 m away from the measuring station, the lateral displacements at 1-2# and 1-1# measuring points increased rapidly, and remained unchanged for a while as the working face continued advancing; when the working face came 24-18 m away from the measuring station, the lateral displacements at 1-1#, 1-2# and 1-3# measuring points increased abruptly, while the lateral displacement at 1-4# saw an initial steep rise; finally, as the working face advanced further, the lateral displacements at 1-1#, 1-2# and 1-3# measuring points all plateaued while the lateral displacement at 1-4# continued climbing.

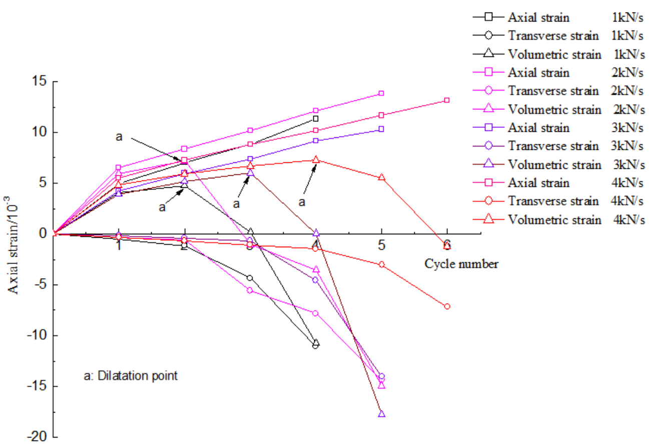

Fig. 11 Relation between strain evolution and cycles number of coal under different loading rates

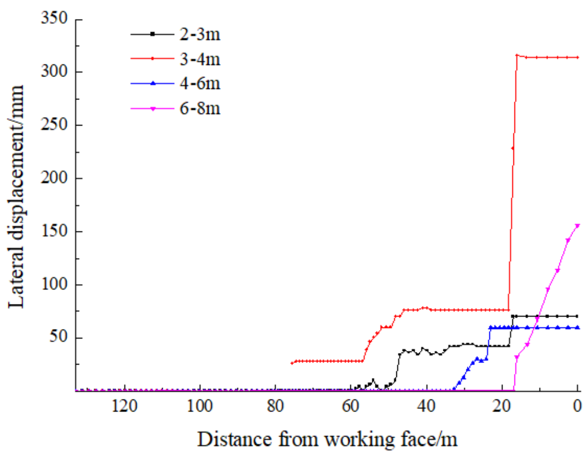

Fig. 12 Variation of the lateral displacements at the measuring points with the advancing of working face

Conclusively, as the distance between the measuring point and the coal walls of working face shrank, the lateral displacement in the shallow coals went through a rise-stabilize-step up-plateau series, while the lateral displacement in deep coals increased steadily. Taking the lateral displacement curve of the coals at the depth of 3-4 m as an example, the relation between the applied force and lateral deformation in different stages was analyzed. At the measuring point 80-62 m away from the working face, lots of pre-existing fractures extended under the mining-induced stress, to give rise to a small lateral displacement. As the working face closed in, the force on the coals at this measuring point intensified gradually and the lateral displacement continued increasing. In this stable failure stage, the lateral displacement would decrease if the external force is reduced. At the measuring point 18 m away from the working face, the lateral displacement increased suddenly in a catastrophic way, indicating the occurrence of severe damage in coals. According to the laboratory test results, this signifies the onset of the dilatation as well as the entry into the accelerated failure stage.

A constant lateral deformation stage can also be observed in monitoring curves, due to the periodical motion of the overburdening strata in coal mining, which induces a periodically changing bearing stress in coals. During the period from the end of one period to the beginning of the next, the stress in the coals in front of the working face at a large distance away remains more or less unchanged; the lateral displacement of the coals in elastic stage remained constant while that in the accelerated stage increased further even under a constant force. However, since the haulageway coals were subjected to supporting and constraint from the adjacent coals, the lateral deformation was restricted and thus the lateral displacement would be constant when the applied force was not enough to produce the stress for further deformation. If a great external force, such as an external dynamic load, was applied, the coals would be further deformed.

The monitoring results demonstrate that the coals at the depth of 2-6 m was severely damaged on account of the action of mining-induced stress; however, the coals in this region didn't see the ultimate failure yet and still held on to a strong deformation resistance, i.e., the coals were in accelerated failure stage; for the coals at the depth over 6 m, the horizontal displacement near the working face increased gradually, but would decrease when the applied force is reduced, i.e., the coals in this region were in stable failure stage.

According to the laboratory test results, the coal rock' lateral deformation can reflect the severity of failure. Therefore, the coals show different lateral deformations at different mining advance speed. With the presence of some dynamic disasters such as rock burst or coal/gas outburst, the internal relation between coal rock's deformation characteristics and dynamic disasters can be constructed based on coal's lateral deformation characteristics for disasters prediction.

4. Conclusions

• Under uniaxial cyclic loading condition, the coal rock showed obvious irreversible lateral deformation before reaching the peak intensity. The coal rock expanded significantly, i.e., an obvious dilatation can be observed; meanwhile, the coal rock's lateral strain was only slightly recovered upon unloading, suggesting that the coal rock had entered the accelerated failure stage.

• In the accelerated failure stage, as the loading rate increased, the coal rock' lateral strain decreased gradually, with a growing change rate. In the post-peak failure stage, the slope of the coal rock's stress-strain curve decreased gradually and the failure tended to be more intensive.

• As the loading rate increased, both the stresses at the dilatation critical point and the ratio of the stress at the dilatation point to peak stress increased gradually. The greater the loading rate, the smaller the volumetric deformation from the dilatation critical point to peak-intensity point.

• Based on laboratory test results, the lateral deformation of the coals in #1302 isolated working face, Yangcheng Coal Mine, was monitored. The monitoring results reveal that the coal lateral displacement is characterized by staged pattern. For the coals at the depth of 2-6 m, the lateral displacement underwent the 'increase-stabilize-step up-plateau series. When the working face was 24-18 m away, the coals at this depth range entered the accelerated failure stage; when the working face was approximately 18 m away, the lateral displacement of the coals at the depth over 6 m increased gradually, i.e., the coals were in the stable failure stage. Accordingly, the failure or instability of coals can be predicted by monitoring their lateral deformations during haulageway tunneling or coal mining process.

Acknowledgements

This work was supported by the Basic Research Project of Qingdao Source Innovation Program (17-1-1-11-jch), the Program of National Natural Science Foundation of Shandong Province (ZR2016EEB07), the Scientific Research Foundation of Shandong University of Science and Technology Talents (2016RCJJ025), Taishan Scholar Talent Team Support Plan for Advantaged& Unique Discipline Areas.

References

Chai, Z., Kang, T. and Chen, W. (2014), "Effects of organic silicone additive material on physical and mechanical properties of mudstone", *Geomech. Eng.*, **6**(2), 139-151.

Chen, S.J., Zhou, H., Guo, W.J., Wang, H.L. and Sun, X.Z. (2012), "Study on long-term stress and deformation characteristics of strip pillar", *J. Min. Safe. Eng.*, **29**(3), 376-380.

Heap, M.J. and Faulkner, D.R. (2008), "Quantifying the evolution of static elastic properties as crystalline rock approaches failure", *J. Rock Mech. Min. Sci.*, **45**(4), 564-573.

Huang, D., Huang, R.Q. and Zhang, Y.X. (2012), "Experimrntal investigations on static loading rate effects on mechanical properties and energy mechanism of coarse crystal grain marble under uniaxial compression", *Chin. J. Rock Mech. Eng.*, **31**(2), 245-255.

Jorat, M.E., Kreiter, S., Moerz, T., Moon, V. and de Lange, W. (2013), “Strength and compressibility characteristics of peat stabilized with sand columns”, *Geomech. Eng.*, **5**(6), 575-594.

Kong, X., Liu, J., Zou, D. and Liu, H. (2016), “Stress-dilatancy relationship of Zipingpu gravel under cyclic loading in triaxial stress states”, *J. Geomech.*, **16**(4), 04016001.

Lyamina, E.A. and Nguyen, T. (2016), “Effect of the yield criterion on the strain rate and plastic work rate intensity factors in axisymmetric flow”, *Struct. Eng. Mech.*, **58**(4), 719-729.

Mouthereau, F., Fillon, C. and Ma, K.F. (2009), “Distribution of strain rates in the Taiwan orogenic wedge”, *Earth Planet. Sci. Lett.*, **284**(3-4), 361-385.

Qi, C., Wang, M. and Qian, Q. (2009), “Strain-rate effects on the strength and fragmentation size of rocks”, *J. Imp. Eng.*, **36**(12), 1355-1364.

Qiu, S.L., Feng, X.T., Xiao, J.Q. and Zhang, C.Q. (2014), “An experimental study on the pre-peak unloading damage evolution of marble”, *Rock Mech. Rock Eng.*, **47**(2), 401-419.

Wang, C.Q., Gao, L.Q. and Chen, S.J. (2013), “Field research on long-term bearing capacity of strip pillar”, *J. Min. Safe. Eng.*, **30**(6), 799-804.

Wang, H.L., Fan, P.X., Wang, M.Y., Li, W.P. and Qian, Y.H. (2011), “Influence of strain rate on progressive failure process and characteristic stresses of red sandstone”, *Rock Soil Mech.*, **32**(5), 1340-1346.

Xiao, J.Q., Ding, D.X., Xu, G. and Jiang, F.L. (2010), “Deformation characteristics of rock under constant amplitude cyclic loading”, *J. Central South Univ. Sci. Technol.*, **41**(2), 685-691.

Xie, Z., Peng, F. and Zhao, T. (2014), “Experimental study on Fatigue crack propagation of fiber metal laminates”, *Steel Compos. Struct.*, **17**(2), 145-157.

Yu, S., Zhu, W.S., Yang, W.M., Zhang, D.F. and Ma, Q.S. (2015), “Rock bridge fracture model and stability analysis of surrounding rock in underground cavern group”, *Struct. Eng. Mech.*, **53**(3), 481-495.

Zhang, J., Yang, J., Han, J. and Zhang, W. (2016), “Evaluation of dilatancy behavior of asphalt mixtures using partial triaxial compression tests”, *J. Mater. Civ. Eng.*, **28**(1), 1-10.

Zhao, W., Huangb, R. and Yanc, M. (2015), “Mechanical and fracture behavior of rock mass with parallel concentrated joints with different dip angle and number based on PFC simulation”, *Geomech. Eng.*, **8**(6), 757-767.

Zhao, X., Cai, M. and Cai, M. (2010), “Considerations of rock dilation on modeling failure and deformation of hard rocks-a case study of the mine-by test tunnel in Canada”, *J. Rock Mech. Geotech. Eng.*, **2**(4), 338-349.

Zhou, J.W., Yang, X.G., Fu, W.X., Xu, J., Li, H.T., Zhou, H.W. and Liu, J. (2010), “Experimental test and fracture damage mechanical characterstic of brittle rock under uniaxial cyclic loading and un loading conditions”, *Chin. J. Rock Mech. Eng.*, **29**(6), 1172-1183.

Zhou, X.P., Yang, H.Q. and Zhang, Y.X. (2009), “Rate dependent critical strain energy density factor of Huanglong limestone”, *Theor. Appl. Fract. Mech.*, **51**(1), 57-61.

CC